



The Effect of the Hydrothermal and Thermal Deactivations on the Adsorptive Properties and Liquid Permeability of a Silica Gel

Hasan Ceylan¹ , Abdullah Devrim Pekdemir² , Müşerref Önal^{3*} ,
and Yüksel Sarıkaya³ 

¹Maltepe University, Faculty of Education, 34857 Maltepe, İstanbul, Turkey

²Graduate School of Natural and Applied Sciences, Ankara University, Ankara, Turkey

³Department of Chemistry, Faculty of Science, Ankara University, Ankara, Turkey

Abstract: Three samples taken from a silica gel Hypersil were hydrothermally treated, washed, and dried under different conditions. The portions from the obtained samples were heated over a temperature range of 300 and 850 °C for 16 h. Surface area and pore volume of all the treated samples were determined respectively by nitrogen adsorption data at 77 K and mercury porosimetry. The volumetric flow rate and permeability of the isopropyl alcohol on the columns filled with the prepared samples were determined depending both the inlet pressure and packing pressure. The optimum conditions to prepare a column filling material with the heights permeability were discussed.

Keywords: Permeability, pore volume, silica gel, surface area, volumetric flow rate.

Submitted: June 15, 2020. **Accepted:** March 01, 2021.

Cite this: Ceylan H, Pekdemir AD, Önal M, Sarıkaya Y. The Effect of the Hydrothermal and Thermal Deactivations on the Adsorptive Properties and Liquid Permeability of a Silica Gel. JOTCSA. 2021;8(2):477-82.

DOI: <https://doi.org/10.18596/jotcsa.753130>.

*Corresponding author. E-mail: onal@science.ankara.edu.tr Tel.: +90 312 21267 20 / 1173, Fax: +90 312 2232395.

INTRODUCTION

Chromatography is a physicochemical analysis method to determine the composition of gaseous and liquid mixtures depending on the difference adsorption/desorption and diffusion rates for their constituents on the compacted porous solids (1-4). The void spaces inside and among the solid particles of internal width less than 2 nm, between 2 and 50 nm, and larger than 50 nm are called micropores, mesopores, and macropores, respectively. Recently, voids of internal width less than 100 nm are named as nanopores (5).

Artificial hydrogels as well as biogenic and volcanic opals are the porous silica polymorphs (6-8). Silica gels have been generally prepared through the selective acid leaching of the silicates such as clay and zeolite minerals (9-11). Also, similar hydrogels have been synthesized by the condensation polymerization of silicic acid (H_4SiO_4). The rate of this reaction changes depending on pH, concentration and temperature (5). Furthermore,

they are derived through base-catalyzed hydrolysis of silanes such as tetramethoxysilane $Si(OCH_3)_4$, tetraethoxysilane, $Si(OC_2H_5)_4$, and silicon tetrachloride, $SiCl_4$ (12-16).

Silica hydrogels have been modified hydrothermal, thermal, aging, and washing at different conditions according to the usage areas such as chromatographic material, adsorbent, catalyst support, and desiccant (17-19). So, the aim of the present study is to evaluate the optimum conditions to obtain a material from a silica gel with the maximum permeability.

MATERIAL AND METHODS

The silica gel used was Hypersil (*H*) 5 μ m (580x8) supplied by Shandon Company, UK. Each of three modified samples and coded as *H1*, *H2*, and *H3* were prepared from 200 g Hypersil through the different treatments as follows. Isopropyl alcohol employed as eluent was supplied from Merck Chemical Company.

H1: Hypersil suspension in an aqueous solution contains 2.5% NH_3 by mass was heated in an autoclave at 175 °C for 22 h, under 10 bar. The hydrothermally aged wet samples were washed with distilled water, dried with a hot airflow, and then stored in a tightly closed plastic bottle.

H2: The same hydrothermal treatment was conducted with the exception that the time was 18 h. Furthermore, the sample was washed with water and acetone, respectively. Then similarly dried and stored.

H3: The hydrothermal treatment was similar but the time was 18.5h. In addition, the aged samples were washed respectively with water, acetone, and dichloroethane and also dried in a rotary evaporator.

The batches from the *H1*, *H2*, and *H3* were heated in a muffle furnace at 300, 500, 640, 700, 770, and 850 °C for 16 h and then stored to use for further experiments.

The specific surface area of the Hypersil and its hydrothermally treated samples *H1*, *H2*, and *H3* as well as their heat treated samples was determined from the nitrogen adsorption data at -196°C, using Brunauer, Emmett, and Teller (BET) method (5, 20). The specific pore volume for the same samples was estimated using Hg-porosimetry under an applied pressure of 40 bar.

The *H1*, *H2*, *H3* and their heated samples at 640°C for 16h were packed into columns 10 cm long and 0.2 cm radius using the slurry-packing method (21-23). Volumetric flow rate ($\dot{v} = dv / dt$) of the isopropylalcohol on the packed columns at 14 bar was measured depending on the inlet pressure which is consecutively increased up to 550 bar.

Similar measurements were carried out using the columns packed 69 bar (p_2) with the unheated *H1*, *H2*, and *H3* samples. The inlet pressure (p_1) was increased step by step up to 550 bar. The \dot{v}_1 value was measured for each p_1 . Each p_1 was affected as packing pressure ($p_2=p_1$) for the latter measurement. However, the applied inlet pressure was removed after each step, then increased up to a constant value of 69 bar (p_1) and \dot{v}_2 value was measured. The corresponding k_1 and k_2 permeabilities were evaluated using the \dot{v}_1 and \dot{v}_2 values.

RESULTS AND DISCUSSION

Adsorptive properties

The specific surface area of Hypersil was found as S (BET- N_2)=251 m^2g^{-1} . The S value for the *H1*, *H2*, and *H3* silica gels as well as their heat treated samples was determined using the same method. Their changes depending on the hydrothermal treatments and their heating temperatures are given in Figure 1. The curves indicate that the specific surface area is greatly decreased by the hydrothermal

treatments. The S value reaches to zero at 850 °C. The *H3* curve is seen more regular than the others.

The specific pore volume of Hypersil was found as $V=0.93 \text{ cm}^3\text{g}^{-1}$ using a Hg-porosimeter under the applied pressure of 40 bar. The V values for the other samples mentioned above were determined by similar a method. Their changes depending on the hydrothermal treatments and their heating temperatures are given in Figure 2. The V values strictly increase by the modification to obtain *H1*, and *H2* samples whereas for *H3* it is not much. The V values reached to zero at 850°C. The most regular curve is for *H3* silica gel. Changes in the S and V values are due to the removing of hydrogen bonded water molecules as well as chemical bonded hydroxyls and silanol groups from the surface of the silica gel particles during the hydrothermal and thermal deactivations.

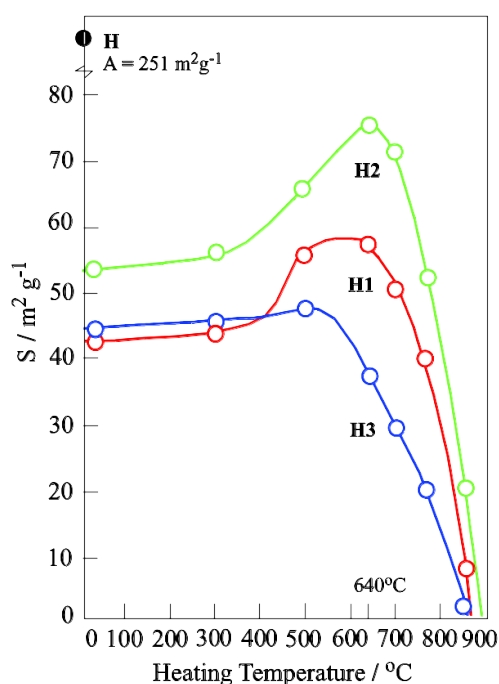


Figure 1. Specific surface area of the Hypersil (*H*), its hydrothermally deactivated samples (*H1*, *H2*, *H3*) and their heated portions.

Volumetric flow rate

Variation of the volumetric flow rate $\dot{v} = (dv / dt)$ of isopropyl alcohol on the columns packed under 14 bar with the *H1*, *H2*, and *H3* samples and their heated portions at 640 °C for 16 h are shown in Figure 3. The irregular curves reveal that the \dot{v} values decrease after the heating of the hydrothermally deactivated samples. The \dot{v} value for *H3* sample is greater than the others at least 20 fold.

The inlet pressure is also affected as a packing pressure on the columns and causes the shrinkage of the samples. Decrease of the length for the *H1*, *H2*, and *H3* columns was found as 4.5, 4.5 and 1.2 cm during the inlet pressure is increased to the 550 bar. On the contrary, shrinkage of the columns

partly decreases the \dot{v} depending on the packed materials. This shrinkage is affected at least the \dot{v} for the *H3* column. So, this sample is more convenient to use as a chromatographic material.

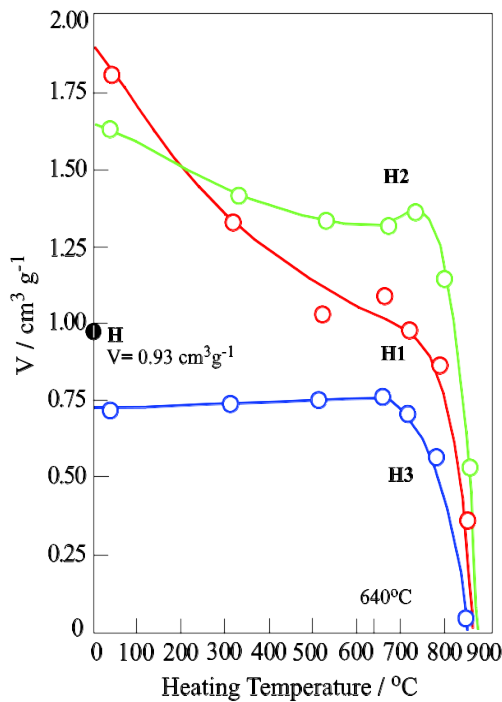


Figure 2. Specific pore volume of the Hypersil (*H*), its hydrothermally deactivated samples (*H1*, *H2*, *H3*) and their heated portions.

The \dot{v} value is defined with the Darcy equation:

$$\dot{v} = k \frac{A p_1}{L \mu} \quad (1)$$

where *A* and *L* are the cross section and length of the filling material inside the column, p_1 is the inlet pressure to the liquid, μ is the viscosity of this liquid and *k* is a proportion coefficient known as permeability. The conditions of

$$\dot{v} / p_1 = kA / \mu = \text{constant} \quad (2)$$

indicates the laminar (viscous) flow according to the fluid mechanics (24). However, the straight lines plotted at the lower values of the inlet pressures show the laminar flows (LF). When the p_1 value is increased the laminar flows disappeared.

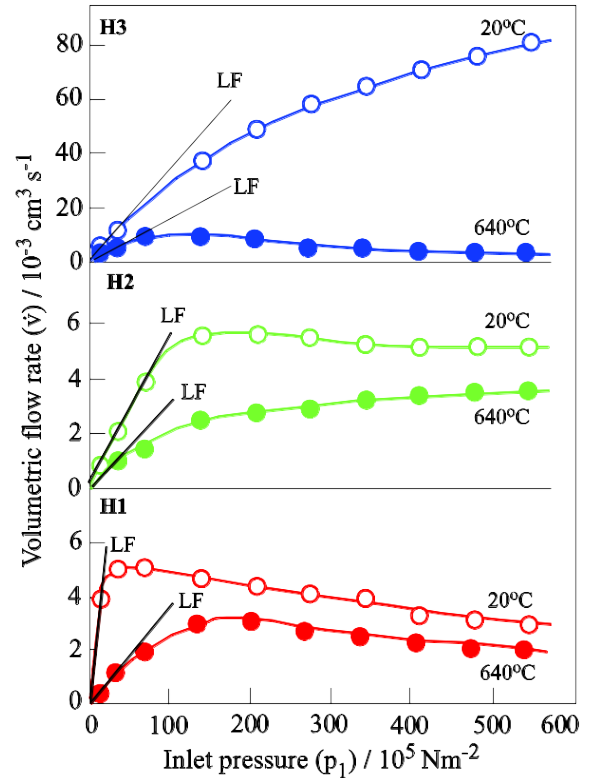


Figure 3. The effect of the inlet pressure on the volumetric flow rate of the isopropyl alcohol on the columns packed at 14 bar using *H1*, *H2*, *H3* and their heated samples.

Permeability

Isopropyl alcohol permeability of the columns can be evaluated from Darcy equation depending on the p_1 and \dot{v} using given column parameters and viscosity (μ) of the eluent. Accordingly, a relationship for the permeability was evaluated in the following form:

$$k (cm^2) = (6.847 \times 10^{-2} Nm^{-2}s) \frac{\dot{v} (cm^3 s^{-1})}{p_1 Nm^{-2}} \quad (3)$$

by taking $\mu = 2.86 \times 10^{-3} Nm^{-2}s$, $r = 0.2$ cm ($A = \pi r^2$), and $L = 10$ cm in the Darcy equation. Permeability-pressure curves are derived from the flow rate-pressure curves.

The change in the permeability of the *H1*, *H2*, and *H3* columns packed at 69 bar with the inlet pressure is given in Figure 4. Accordingly, the *H3* column has the heights permeability among the three columns. Also, its change rate with the inlet pressure is lower than the others.

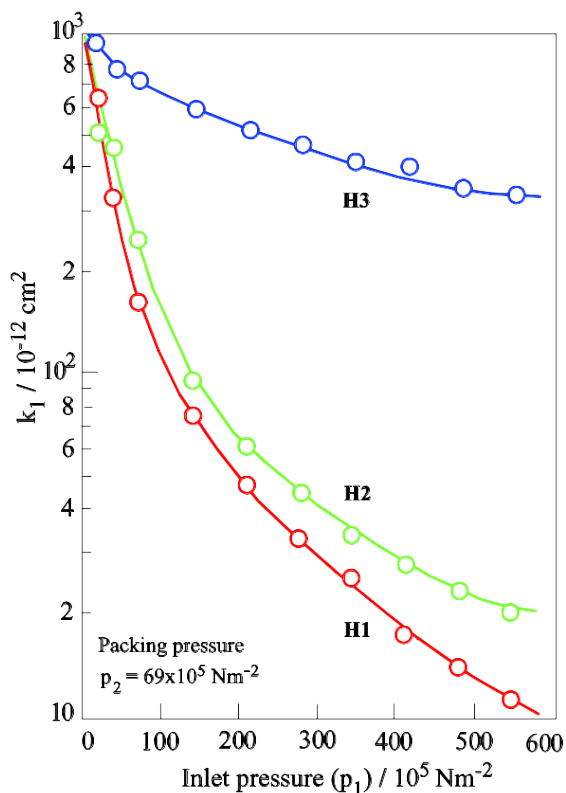


Figure 4. The effect of the inlet pressure on the permeability for the isopropyl alcohol on the *H1*, *H2*, and *H3* columns packed at 69 bar.

The change in the permeability of the same columns with the packing pressure at a constant inlet pressure of 69 bar is shown in Figure 5. A decrease in the permeability with the increasing of the packing pressure at a constant inlet pressure of 69 bar is much more than that inlet pressure. This difference is due to the effect of the inlet pressure during the first measurement as a packing pressure for the second measurement. Accordingly, the change rate of the permeability with the packing pressure increases in the order of *H1*, *H2*, and *H3* samples. This result also shows that the *H3* sample is more convenient packed material for the chromatography columns.

CONCLUSION

Change in the chromatographic properties of the hydrothermally and thermally deactivated porous solid may be generally examined through surface area, pore volume, and particle size determination. These physicochemical properties can be arranged to the desired aspect by change in the deactivation parameters such as temperature, time, washing, material and drying process. The fluid permeability of the treated samples was determined. Fluid permeability on the columns packed with the treated solids was examined with respect to the column packing pressure and inlet pressure for the flow. The sample with the heights permeability is selected as a chromatographic material.

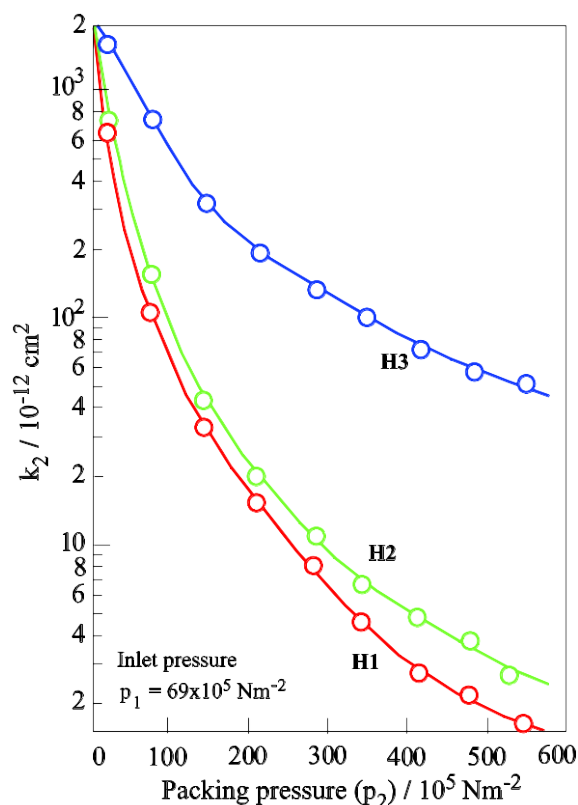


Figure 5. The effect of the packing pressure on the permeability of isopropyl alcohol on the *H1*, *H2*, *H3* columns at the constant inlet pressure of 69 bar.

ACKNOWLEDGMENTS

The authors are thankful to the Edinburgh University for experimental support and the Ankara University Research Fund (Project No:16L043013) for financial support to this work.

REFERENCES

1. Scott RPW, Kucera P. Some aspect of the chromatographic properties of thermally modified silica gel. *Journal of Chromatographic Science* 1975;13:337-43.
2. Du Fresne von Hohenesche C, Ehwald V, Unger KK. Development of standard operation procedures for the manufacture of n-octadecyl bonded silicas as packing material in certified reference columns for reserved-phase liquid chromatography. *Journal of Chromatography A* 2004;1025:177-87.
3. Skudas R, Grimes BA, Thommes M, Unger KK. Flow-through pore characteristics of monolithic silicas and their impact on column performance in high-performance liquid chromatography. *Journal of Chromatography A* 2009;1216:2625-36.
4. Shirasaka H, Shimonosono T, Hirata Y, Sameshima S. Analysis of gas permeability of porous alumina powder compacts. *Journal of Asian Ceramic Societies* 2013;1:368-73.

5. Rouquerol F, Rouquerol J, Sing KSW, Llewellyn P, Maurin G. Adsorption by powders and porous solids. Elsevier; 2014.
6. Choi J, Fujita H, Ogura M, Sakoda A. Confinement effect on enthalpy of fusion and melting point of organic phase change materials in cylindrical nanoscape of mesoporous silica and carbon. Adsorption 2018;24:345-55.
7. Ding H, Li J, Gao Y, Zhao D, Shi D, Mao G, Liu S, Tan X. Preparation of silica nanoparticles from waste silicon sludge. Powder Technology 2015;284:231-6.
8. Li J, Xu L, Zheng N, Wang H, Lu F, Li S. Biomimetic synthesized bimodal nanoporous silica: Bimodal mesostructure formation and application for ibuprofen delivery. Materials Science and Engineering C 2016;58:1105-11.
9. Temuujin J, Okada K, MacKenzie KJD. Preparation of porous silica from vermiculite by selective leaching. Applied Clay Science 2003;22:187-95.
10. Hu X, Yan X, Zhou M, Komarneni S. One-step synthesis of nanostructured mesoporous ZIF-8/silica composites. Microporous and Mesoporous Materials 2016;219:311-6.
11. Krasucka P, Stefaniak W, Kierys A, Goworek J. One-pot synthesis of two different highly porous silica materials. Microporous and Mesoporous Materials 2016;221:14-22.
12. Lee BI, Quesnel E. Low density silica gels and solvent permeability. Journal of the European Ceramic Society 1998;18:123-9.
13. Klotz M, Ayrál A, Guizard C, Cot L. Synthesis and characterization of silica membranes exhibiting an ordered mesoporosity. Control of the porous texture and effect on the membrane permeability. Separation and Purification Technology 2001;25:71-8.
14. Azzouz I, Essoussi A, Fleury J, Haudebourg R., Thiebaut D, Vial J. Feasibility of the preparation of silica monoliths for gas chromatography: Fast separation of light hydrocarbons. Journal of Chromatography A 2015;1383:127-33.
15. Beygi H, Karimi EZ, Farazi R, Ebrahimi F. A statistical approach to synthesis of functionally modified silica nanoparticles. Journal of Alloys and Compounds 2016;654:308-14.
16. Kato N, Kato N. High-yield hydrothermal synthesis of mesoporous silica hollow capsules. Microporous and Mesoporous Materials 2016;219:230-9.
17. Scherer GW. Effect of drying on properties of silica gel. Journal of Non-Crystalline Solids 1997;215:155-68.
18. Gunawan S, Ismadji S, Ju Y-H. Design and operation of a modified silica gel column chromatography. Journal of the Chinese Institute of Chemical Engineers 2008;39:625-33.
19. Mignot M, Sebban M, Tchaplá A, Mercier O, Cardinael P, Peulon-Agasse V. Thermal pretreatments of superficially porous silica particles for high-performance liquid chromatography: Surface control, structural characterization and chromatographic evaluation. Journal of Chromatography A 2015;1419:45-57.
20. Sarıkaya Y, Ceylan H, Önal M, Pekdemir AD. Thermal deactivation kinetics and thermodynamics of a silica gel using surface area data. Journal of Thermal Analysis and Calorimetry 2021;doi.org/10.1007/s10973-020-10132-z.
21. Cherrak DE, Al-Bokari M, Drumm EC, Guiochon G. Behavior of packing materials in axially compressed chromatographic columns. Journal of Chromatography A 2001;943:15-31.
22. Núñez O, Nakanishi K, Tanaka N. Preparation of monolithic silica columns for high-performance liquid chromatography. Journal of Chromatography A 2008;1191:231-52.
23. Hara T, Makino S, Watanabe Y, Ikegami T, Cabrera K, Smarsly B, Tanaka N. The performance of hybrid monolithic capillary columns prepared by changing feed ratios of tetramethoxysilane and methyltrimethoxysilane. Journal of Chromatography A 2010;1217:89-98.
24. Anisah S, Kanezashi M, Nagasawa H, Tsuru T. Hydrothermal stability and properties of TiO₂-ZrO₂ (5/5) nanofiltration membranes at high temperatures. Separation and Purification Technology 2019; 212:1001-12.

